Earth and Planetary Science Letters 357–358 (2012) 277–288

Contents lists available at SciVerse ScienceDirect

Earth and Planetary Science Letters

journal homepage: www.elsevier.com/locate/epsl

Calibration and application of the branched GDGT temperature proxy on East African lake sediments

Shannon E. Loomis [a,*], James M. Russell [a], Bethany Ladd [a], F. Alayne Street-Perrott [b], Jaap S. Sinninghe Damsté [c,d]

[a] Brown University, Department of Geological Sciences, 324 Brook St., Box 1846, Providence, RI 02912, United States
[b] Department of Geography, College of Science, Swansea University, Singleton Park, Swansea SA32 7QD, United Kingdom
[c] NIOZ Royal Netherlands Institute for Sea Research, Department of Marine Organic Biogeochemistry, PO Box 59, 1790 AB Den Burg, Texel, The Netherlands
[d] University of Utrecht, Department of Geosciences, PO Box 80.021, 3508 TA Utrecht, The Netherlands

ARTICLE INFO

Article history:
Received 8 March 2012
Received in revised form
6 September 2012
Accepted 20 September 2012
Editor: J. Lynch-Stieglitz
Available online 24 October 2012

Keywords:
glycerol dialkyl glycerol tetraether
paleothermometer
lake sediment
temperature
Africa
climate

ABSTRACT

Branched glycerol dialkyl glycerol tetraethers (brGDGTs) are a novel proxy for mean annual air temperature (MAAT) and have the potential to be broadly applicable to climate reconstruction using lacustrine sediments. Several calibrations have been put forth relating brGDGT distributions to MAAT using a variety of linear regressions, including the methylation (MBT) and cyclization (CBT) indices of brGDGTs, the relative abundances of the major, non-cyclized brGDGTs (MbrGDGTs), and best subsets regression (BSR) of the fractional abundances of the nine most common brGDGTs. However, these calibrations have rarely been applied to lake sediment cores to reconstruct temperatures and test the applicability of this proxy as a paleothermometer.

We present an expanded East African lakes surface sediment brGDGT dataset based upon 111 lakes and examine three methods of calibrating brGDGTs to MAAT. These methods include recalculations of the East African lake MBT/CBT calibration and MbrGDGTs calibrations, as well as a new stepwise forward selection (SFS) calibration that uses the four combined brGDGTs that explain the most variance in temperature in our calibration set. We apply these new calibrations as well as five previously published lacustrine brGDGT calibrations to the brGDGT distributions of our surface sediment dataset and a 48 kyr sediment core from Sacred Lake, Mt. Kenya, producing the first brGDGT temperature reconstruction available from a small tropical lake. We compare the reconstructed temperatures to previously published paleotemperature records from East Africa to help us assess the performance of the brGDGT calibrations. We find that the SFS calibration has a consistently low root mean squared error of prediction (RMSEP) over the entire range of MAAT, while the MBT/CBT and MbrGDGT calibrations have relatively large RMSEPs, particularly between lakes with similar temperatures but variable pH. This suggests that these techniques do not properly deconvolve the temperature and pH signals recorded in the distributions of the brGDGTs. We further find that only the SFS calibration produces a credible reconstructed temperature history from Sacred Lake when compared to other last glacial maximum paleotemperature estimates from East Africa. Thus, we advocate for the use of the SFS calibration when reconstructing paleotemperatures from brGDGTs in East Africa.

1. Introduction

Over 40 years of research have provided a regionally coherent view of tropical African paleohydrology from the last glacial maximum (LGM) to the present (Gasse et al., 2008 and references therein), but we know virtually nothing of the thermal history of tropical Africa, as we lack quantitative proxies for air temperature in the tropics. As such, high-resolution, quantitative paleotemperature records are necessary to constrain the full range of natural temperature variations and the processes governing long-term temperature changes on the tropical continents.

Abbreviations: brGDGT, Branched glycerol dialkyl glycerol tetraether; BSR, Best subsets regression; CBT, Cyclisation ratio of branched tetraethers; ELA, Equilibrium line altitude; GDGT, Glycerol dialkyl glycerol tetraether; lakes $_{<16}$, Lakes with a MAAT under 16 °C; LGM, Last glacial maximum; LST, Lake surface temperature; MAAT, Mean annual air temperature; MbrGDGT, Major branched glycerol dialkyl glycerol tetraether; MBT, Methylation index of branched tetraethers; MSAT; Mean summer air temperature; RMSE, Root mean squared error; RMSEP, Root mean squared error of prediction; SFS, Stepwise forward selection; TEX_{86}, Tetraether index of 86 carbon atoms

* Corresponding author. Tel.: +1 401 863 2810; fax: +1 401 863 2058.
E-mail address: Shannon_Loomis@brown.edu (S.E. Loomis).

0012-821X/$ - see front matter © 2012 Elsevier B.V. All rights reserved.
http://dx.doi.org/10.1016/j.epsl.2012.09.031

Until recently, virtually all temperature reconstructions from tropical Africa provided only "time-slice" estimates of the degree of cooling during the LGM relative to the present. These data show that the LGM was cooler than today, but with considerable uncertainty regarding its amplitude. For instance, pollen-based estimates (Bonnefille et al., 1990; Coetzee, 1967), noble gas analyses of fossil aquifers (Kulongoski et al., 2004; Stute and Talma, 1998), and equilibrium line altitude (ELA) estimates deduced from mountain glacier moraines (Mark et al., 2005) suggest a mean warming of 2–8 °C from the LGM to the pre-industrial period. More recently, the development and application of the TEX_{86} (TetraEther indeX of 86 carbon atoms; Schouten et al., 2002) and the MBT/CBT (methylation index of branched tetraethers/cyclization index of branched tetraethers; Weijers et al., 2007b) paleothermometers to sediment cores from Lake Malawi (Powers et al., 2005), Lake Tanganyika (Tierney et al., 2008), and the Congo Fan (Weijers et al., 2007a) have expanded our understanding of Africa's thermal history by providing continuous temperature records dating back past the LGM. These data confirm LGM-present warming but with large differences in the timing and dynamics of temperature change since the LGM. The disparities among these records could derive from regional and/or altitudinal effects, which are hard to evaluate given the limited number of sites. Moreover, existing paleotemperature estimates are derived from a variety of proxies, which each have their own sources of error and assumptions. For example, both vegetation changes (Street-Perrott et al., 1997) and glacial ELA (Mark et al., 2005) estimates are sensitive to a number of climate variables beyond temperature, while TEX_{86} is only applicable in a limited number of large lakes (Powers et al., 2010) with potentially complex mixing regimes (Berke et al., 2012; Sinninghe Damsté et al., 2012).

Branched glycerol dialkyl glycerol tetraethers (brGDGTs, Fig. 1) have the potential to be a universal paleotemperature proxy. BrGDGTs are ubiquitous in peats (Weijers et al., 2006), soils (Weijers et al., 2007b), ocean sediments (Weijers et al., 2007a), and lake sediments (Blaga et al., 2010; Pearson et al., 2011; Sun et al., 2011; Tierney et al., 2010). Weijers et al. (2007b) first demonstrated that variations in the distributions of the nine brGDGTs could be correlated to environmental conditions in globally distributed soils and developed calibrations to mean annual air temperature (MAAT) and soil pH based on the number of methyl branches (MBT) and cyclopentyl moieties (CBT) in brGDGT alkyl chains. A few studies have used this soil-based calibration to reconstruct MAAT in ocean margin sediments (Weijers et al., 2007a), loess (Peterse et al., 2011), and lake sediments (Fawcett et al., 2011).

Numerous investigations have demonstrated significant differences between the distributions and concentrations of brGDGTs in lake sediments and the surrounding soils (Loomis et al., 2011; Sinninghe Damsté et al., 2009; Tierney and Russell, 2009) and find that soil-based calibrations (Weijers et al., 2007b) do not accurately reconstruct MAAT from most lake surface sediments (Blaga et al., 2010; Sun et al., 2011; Tierney et al., 2010). Various mechanisms have been invoked to explain these differences, including seasonal temperature bias and production within lakes. Although Weijers et al. (2011) found a lack of seasonal variability in the distributions of brGDGTs when sampling soils at different times of year, lacustrine systems may behave differently than soils with regard to seasonal biases, as soils build up brGDGTs in situ while lake sediment brGDGTs should be derived, at least in part, from settling particles. Regardless, seasonal temperature variability is minimal in the tropics, as are offsets between mean annual lake and air temperatures, so in situ production is the likely cause of this soil/lake sediment offset in East Africa (Loomis et al., 2011; Tierney et al., 2010). To correct for these differences, Tierney et al. (2010) calculated two new MAAT calibrations using brGDGT distributions in 41 East African lake sediments: one based upon the MBT and CBT indices, and a second utilizing the fractional abundances of the three most abundant, non-cyclized brGDGTs, the so-called "major" brGDGTs (MbrGDGTs). Subsequent work has built upon these studies using various lake sediment training sets. Sun et al. (2011) combined new data from Chinese lakes with previously published lacustrine brGDGT data to create a global MBT/CBT calibration. Pearson et al. (2011) utilized lake sediments from the Arctic to Antarctica to calculate a calibration based on the MbrGDGTs and further developed a new calibration that used best subsets regression (BSR) on the fractional abundances of brGDGTs.

As of yet, none of these lake calibrations have been successfully applied to reconstruct paleotemperatures from a lake sediment core, and these calibrations have not been systematically tested using a single set of lake surface sediment samples. Here we expand the East African lakes calibration data set by adding 70 new sites to the 41 sites published by Tierney et al. (2010). We use these data to create three new calibrations: two based on recalculation of the MBT/CBT and MbrGDGTs calibrations and a third utilizing stepwise forward regression (SFS; Hocking, 1976). We apply both the previously published and new lacustrine brGDGT temperature calibrations to our surface sediment dataset and to a 48 kyr sediment core from Sacred Lake, Mt. Kenya to assess the validity of each of the calibrations in comparison with published records of temperature change over equatorial Africa since the LGM.

2. Methods

2.1. Field sampling and study sites

Here we augment a previously published 41-sample lacustrine brGDGT dataset from East Africa (Tierney et al., 2010) with 70 new lake surface sediment samples collected between 1996 and 2010 (Fig. 2, Table A1). New samples are mostly from Mt. Kenya and western Uganda where there are numerous lakes at different elevations over relatively small areas. As a glaciated stratovolcano, Mt. Kenya contains both crater and glacial lakes along its flanks, ranging from 2350 to 4752 m above sea level (asl).

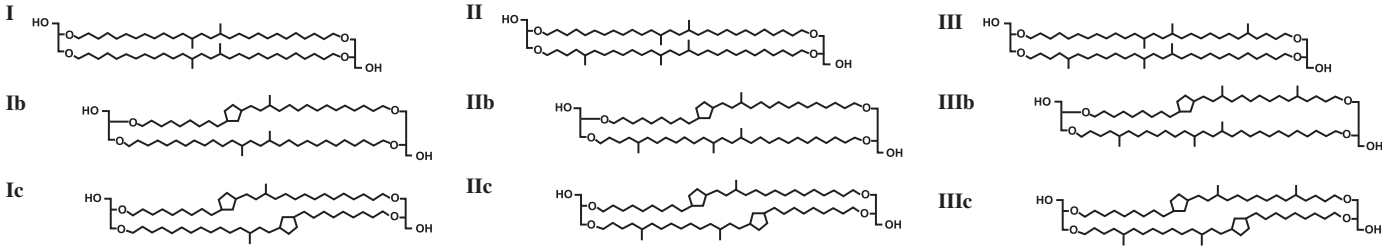

Fig. 1. Structures of the brGDGTs discussed in the text.

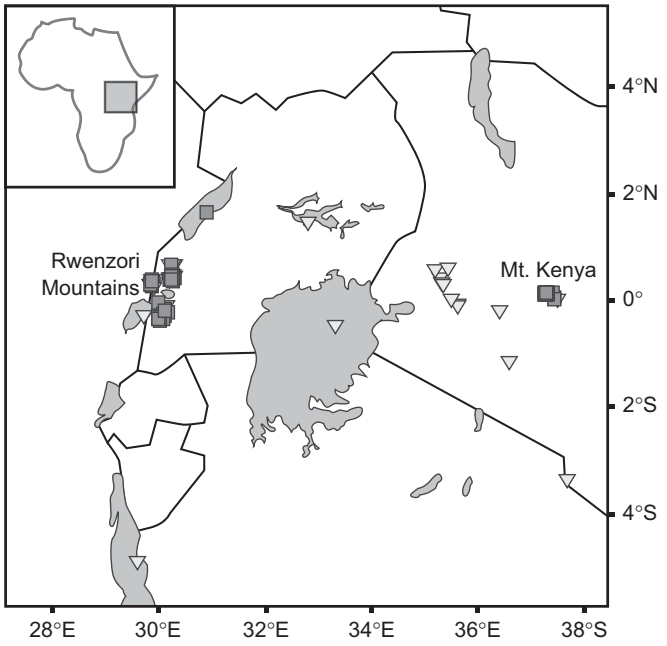

Fig. 2. Map of locations of lake surface sediments for the expanded East African lakes dataset. Triangles are locations of sites from Tierney et al. (2010) and squares are sites from this study.

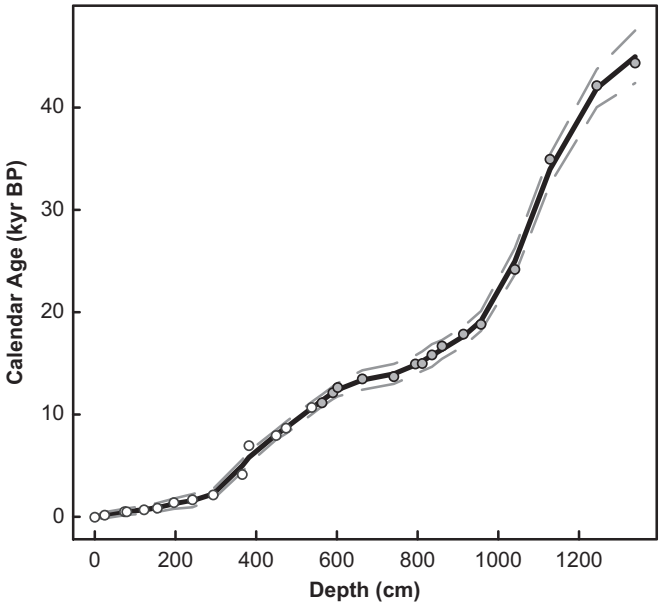

Fig. 3. Calendar age (BP) vs. depth (cm) for the Sacred Lake core (SL1). Open circles are new ages presented here, and gray circles are data from Olago et al. (2001).

Western Uganda houses numerous lakes in the Kasenda Crater Lake District (925 to 1735 m asl) and the Rwenzori Mountains (2990 to 4487 m asl). MAAT at each site was calculated from previously published lapse rates for both regions (Eggermont et al., 2010). In the 41-lake surface sediment dataset of Tierney et al. (2010), MAAT and pH were strongly positively correlated. We therefore targeted cold lakes with high pH to reduce the covariance of these environmental variables.

The sediment core used in this study was collected from Sacred Lake, Mt. Kenya (0°05′N, 37°32′E, 2350 m asl; Street-Perrott et al., 1997). Sacred Lake is a closed maar lake formed by a basaltic explosion and had a maximum depth of 5 m at the time of coring. The 16.34 m long core (SL1) was obtained using a Livingstone corer at 2.5 m water depth. Upon opening, the core was cut into continuous, 1 cm increments, which were sealed in plastic Petri dishes and stored at 4 °C. The bottom 1.5 m of core is a silty diamict with pumice and organic clasts, which transitions into smooth organic mud for the next 10.5 m. The top 4 m of the core consist of organic mud with abundant plant macrofossils. The upper 14.5 m of core are interrupted by cm-scale ash layers and peat layers that were not sampled for the brGDGT reconstruction due to the potential for soil-derived brGDGT contamination.

We analyzed 93 SL1 core samples at a 15 cm average resolution between 0.12 and 14.43 m core depth (mcd). The new age model for SL1 presented here (Fig. 3, Table A2) is derived from 29 radiocarbon dates (15 from Olago et al., 2001, 14 previously unpublished) calibrated to calendar years using Calib 6.0 (Stuiver and Reimer, 2010) and interpolated using mixed-effect regression (Heegaard et al., 2005).

2.2. Analysis of brGDGTs

All calibration and core samples were freeze dried at Brown University, homogenized, and the lipids extracted from 0.02 to 2.2 g of sediment with 9:1 dichloromethane:methanol (DCM:MeOH, v/v) using a Dionex 350 accelerated solvent extractor (ASE). Separation and quantification of brGDGTs was achieved using the methods of Huguet et al. (2006). Surface sediment samples were analyzed at the Royal Netherlands Institute for Sea Research (NIOZ), and Sacred Lake core samples were analyzed at Brown University. BrGDGTs were quantified by integration of the peak areas as defined by Weijers et al. (2007b). Ten percent of the samples were run in duplicate to check for reproducibility. Average duplicate error was 0.0004 for GDGT fractional abundances, 0.001 for MBT, and 0.002 for CBT.

2.3. Mathematical and statistical analysis

The MBT and CBT indices were calculated according to Weijers et al. (2007b), whereby

$$\mathrm{MBT} = [\mathbf{I}+\mathbf{Ib}+\mathbf{Ic}]/[\mathbf{I}+\mathbf{Ib}+\mathbf{Ic}+\mathbf{II}+\mathbf{IIb}+\mathbf{IIc}+\mathbf{III}+\mathbf{IIIb}+\mathbf{IIIc}] \quad (1)$$

$$\mathrm{CBT} = -\log([\mathbf{Ib}+\mathbf{IIb}]/[\mathbf{I}+\mathbf{II}]) \quad (2)$$

and **I**, **Ib**, etc. refer to the structures identified in Fig. 1. The fractional abundance, $f(i)$, of each brGDGT, i, is defined as

$$f(i) = i/[\mathbf{I}+\mathbf{Ib}+\mathbf{Ic}+\mathbf{II}+\mathbf{IIb}+\mathbf{IIc}+\mathbf{III}+\mathbf{IIIb}+\mathbf{IIIc}] \quad (3)$$

where i varies from **I**, **Ib**, etc.

Outliers for all calibrations were identified iteratively as data whose residuals were more than three standard deviations away from the mean and were excluded from error calculations. Outliers were not incorporated when calculating new calibrations.

The root mean squared error of prediction (RMSEP) was calculated for new and previously published calibrations using our surface sediment dataset. We also determined the maximum (max) bias of each calibration by ordering our data by observed MAAT, dividing the data into 10 intervals of equal sample size, calculating the average of the residuals in each interval, and taking the maximum absolute value of those 10 averages (ter Braak and Juggins, 1993). We further calculated the RMSE of lakes with MAAT below 16 °C ($\mathrm{lakes}_{<16}$) and above 16 °C ($\mathrm{lakes}_{>16}$) to determine model performance at different temperature ranges.

Cross validation was performed using bootstrapping with 1000 resamples and applied to the Sacred Lake reconstructions to determine reconstructed temperature errors (Efron, 1979) for all new calibrations along with the calibrations of Tierney et al. (2010) and Sun et al. (2011). Reported temperature changes in

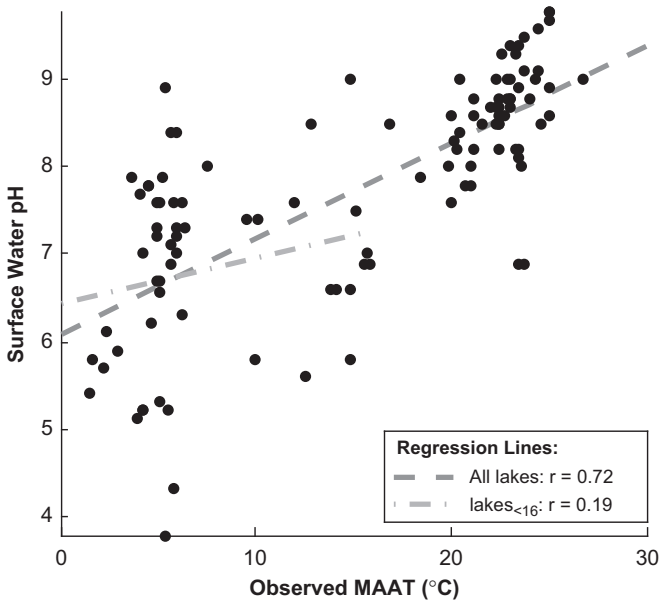

Fig. 4. Surface water pH vs. MAAT for the lakes in our calibration. Dashed line shows the correlation between pH and MAAT for all sites ($r=0.72$); dot-dashed line shows the correlation between pH and MAAT for MAAT <16 °C ($r=0.19$).

Sacred Lake between the LGM, mid-Holocene, and present are calculated from a 5-point running mean to capture broader thermal trends.

3. Results

3.1. Lake surface sediment dataset

Our new dataset combined with the data of Tierney et al. (2010) contains sediments from 111 East African lakes, which span over 1 km in depth, 25 °C in MAAT, and 6 pH units in the surface waters (Fig. 4, Table A1). Correlation between all three of these environmental variables is significant ($p<0.001$ for all pairs). MAAT and pH have the highest correlation ($r=0.72$, Fig. 4), but correlation varies within the dataset. An *F*-test shows that the largest break in the variance of the MAAT/pH relationship occurs at 16 °C; lakes$_{<16}$ exhibit no significant relationship between MAAT, pH, and depth ($p>0.05$ for all pairs). Because of this, we analyze correlations and calibration misfit over the lake$_{<16}$ sites as well as the entire suite of East African lakes.

Non-cyclized brGDGTs from our new samples have a mean fractional abundance of 0.820 ($\sigma=0.145$). The mean fractional abundances of brGDGTs with one and two cyclopentane rings are 0.158 ($\sigma=0.051$) and 0.021 ($\sigma=0.008$), respectively. The mean MBT value is 0.373 ($\sigma=0.153$), and the mean CBT value is 0.749 ($\sigma=0.376$).

Correlations between fractional abundances of brGDGTs and MAAT across the entire combined dataset vary widely (Table 1a); **III** has the highest absolute correlation with MAAT ($r=-0.89$, $p<0.001$), while **IIc** has the lowest ($r=0.01$, $p=0.93$). Furthermore, **I** and **Ib** are both significantly correlated to MAAT ($p<0.001$), with r values of 0.85 and 0.77, respectively. In the lakes$_{<16}$ dataset (Table 1b), **III** and **I** remain highly correlated to MAAT ($r=-0.80$ and 0.78, respectively; $p<0.001$), while the correlation between MAAT and **Ib** is less significant ($r=0.30$, $p=0.03$).

Surface water pH correlates most closely with **Ib** ($r=0.74$, $p<0.001$) in our dataset, and depth has low ($|r|\leq 0.44$) but significant ($p\leq 0.03$) correlation with all brGDGTs except **I** and **IIIb** (Table 1a). In the lakes$_{<16}$ dataset (Table 1b), pH is most

Table 1
Correlation coefficients and *p* values for the nine brGDGTs and environmental variables, including MAAT (°C), surface water pH (SW pH), and depth (m) for (a) the entire lakes dataset and (b) the lakes$_{<16}$ dataset.

		III	IIIb	IIIc	II	IIb	IIc	I	Ib	Ic
(a) All lakes										
MAAT	*r*	−0.89	0.08	0.22	−0.54	0.46	0.01	0.77	0.85	0.54
	p	<0.001	0.394	0.023	<0.001	<0.001	0.931	<0.001	<0.001	<0.001
SW pH	*r*	−0.63	0.41	0.20	−0.41	0.63	0.19	0.34	0.74	0.49
	p	<0.001	<0.001	0.032	<0.001	<0.001	0.043	<0.001	<0.001	<0.001
Depth	*r*	−0.30	0.11	0.30	−0.21	0.36	0.24	0.10	0.44	0.36
	p	0.001	0.239	0.001	0.031	<0.001	0.013	0.318	<0.001	<0.001
(b) Lakes$_{<16}$										
MAAT	*r*	−0.80	−0.12	−0.16	0.15	−0.02	−0.11	0.78	0.30	0.09
	p	<0.001	0.403	0.234	0.278	0.907	0.432	<0.001	0.030	0.539
SW pH	*r*	−0.23	0.49	−0.03	0.03	0.51	0.31	−0.17	0.48	0.38
	p	0.092	<0.001	0.849	0.845	<0.001	0.021	0.210	<0.001	0.005
Depth	*r*	0.24	0.19	0.15	−0.07	0.08	0.18	−0.29	−0.02	0.07
	p	0.080	0.169	0.282	0.603	0.550	0.196	0.031	0.888	0.597

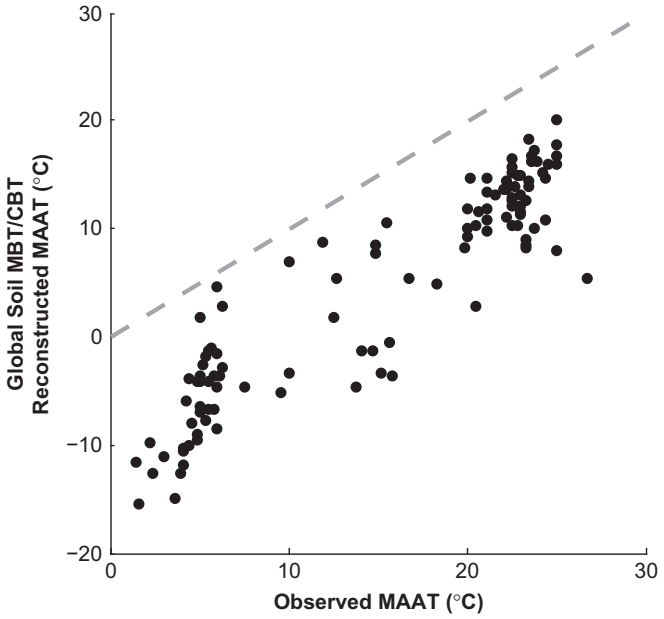

Fig. 5. Global soils MBT/CBT calibration applied to our surface sediment dataset. Surface sediment samples are plotted in black dots, with a 1:1 dashed gray line for reference.

significantly correlated with the brGDGTs with one cyclopentyl moiety ($0.48 < r < 0.51$, $p < 0.001$ for all), while only brGDGT **I** has a significant correlation with depth ($r = -0.29$, $p = 0.03$).

3.2. Application of previously published calibrations to the new East African surface samples

We applied previously published brGDGT calibrations to our surface sediment dataset, including the global soils MBT/CBT calibration (Weijers et al., 2007b), the original East African MBT/CBT and MbrGDGT calibrations (Tierney et al., 2010), the global MBT/CBT calibration (Sun et al., 2011), and the global MbrGDGT and BSR calibrations (Pearson et al., 2011). It should be noted that Pearson et al. (2011) calibrated their models to mean summer air temperature (MSAT) instead of MAAT; however, all lakes examined in this study experience seasonal temperature variability < 2 °C (McGregor and Nieuwolt, 1998). As this is less than the root mean squared error (RMSE) on both of the Pearson et al. (2011) calibrations, the reconstructed MSAT from these calibrations should be equivalent to MAAT for our analysis of model performance.

When we apply the global soil MBT/CBT calibration (Weijers et al., 2007b):

$$\mathrm{MAAT} = -6.10 + 50.00 \times \mathrm{MBT} - 9.35 \times \mathrm{CBT} \quad (4)$$

to our surface sediment dataset (Fig. 5), all reconstructed MAAT values are below the observed MAAT for those sites. The two lacustrine MBT/CBT calibrations, however, reconstruct MAAT more accurately. The original East African lakes MBT/CBT calibration (Tierney et al., 2010), defined as:

$$\mathrm{MAAT} = 11.84 + 32.54 \times \mathrm{MBT} - 9.32 \times \mathrm{CBT} \quad (5)$$

had an r^2 value of 0.89 and a RMSE of 3.0 °C, but when we apply this calibration to our new lake surface sediments, the RMSEP rises to 3.6 °C with a max bias of 4.2 °C (Fig. 6a, Table 2). Conversely, application of the Sun et al. (2011) calibration:

$$\mathrm{MAAT} = 6.80 + 37.09 \times \mathrm{MBT} - 7.06 \times \mathrm{CBT} \quad (6)$$

to our surface sediment samples decreases the RMSE from 5.2 °C to a RMSEP of 3.2 °C, with a max bias of 3.0 °C (Fig. 6b, Table 2). Both of these calibrations show the highest variability in reconstructed MAAT at the lake $_{<16}$ sites.

Two lacustrine brGDGT temperature calibrations are based solely on MbrGDGTs to account for the dependence of the cyclized brGDGTs on environmental parameters other than MAAT (Pearson et al., 2011; Tierney et al., 2010). The original East African MbrGDGTs calibration (Tierney et al., 2010):

$$\mathrm{MAAT} = 50.47 - 74.18 \times f(\mathbf{III}) - 31.60 \times f(\mathbf{II}) - 34.69 \times f(\mathbf{I}) \quad (7)$$

had an r^2 of 0.94 and an RMSE of 2.2 °C when applied to 41 East African lakes; however, the performance of this calibration decreases when applied to our surface sediment dataset, with a RMSEP of 3.0 °C and max bias of 3.7 °C (Fig. 7a, Table 2). The global MbrGDGT calibration (Pearson et al., 2011) is regressed against MSAT:

$$\mathrm{MSAT} = 47.4 - 53.5 \times f(\mathbf{III}) - 37.1 \times f(\mathbf{II}) - 20.9 \times f(\mathbf{I}) \quad (8)$$

and performs more poorly than the East African MbrGDGTs calibration when applied to our data, with a RMSEP of 4.4 °C and max bias of 6.8 °C (Fig. 7b, Table 2). Again, both MbrGDGT calibrations show highest variability lake $_{<16}$ sites.

Pearson et al. (2011) also proposed a global best subsets regression (BSR) calibration based upon linear regression of the fractional abundance of brGDGTs **Ib**, **II**, and **III** in lake sediments on MSAT:

$$\mathrm{MSAT} = 20.9 - 20.5 \times f(\mathbf{III}) - 12.0 \times f(\mathbf{II}) + 98.1 \times f(\mathbf{Ib}) \quad (9)$$

Their calibration has an r^2 of 0.88 and a RMSE of 2.0 °C. Using our surface sediment dataset, the model error increases, with an RMSEP of 5.1 °C and max bias of 6.6 °C (Fig. 8a, Table 2). Again, the model precision decreases at lake $_{<16}$ sites, and like the global MbrGDGTs calibration (Pearson et al., 2011), the BSR calibration exhibits significant bias toward warm temperature at our cold sites.

3.3. Application of previously published calibrations to Sacred Lake core sediments

To test the performance of previously published brGDGT calibrations as a paleothermometer, we apply them to our core samples from Sacred Lake and evaluate temperature changes between the LGM (the reconstructed temperature minimum at 22 ka), mid-Holocene (the reconstructed temperature maximum at 7 ka), and present (pre-industrial). The original East African lakes MBT/CBT calibration (Tierney et al., 2010) shows warming of 3.8 °C from the LGM into the mid-Holocene, followed by a sharp cooling of 4.8 °C, eliminating the temperature rise during the glacial termination (Fig. 6d, Table 2). Application of the global MBT/CBT calibration (Sun et al., 2011) shows a similar pattern to that of the original East African MBT/CBT calibration (Tierney et al., 2010), with steady warming from the LGM to the mid-Holocene ($\Delta T = 6.6$ °C), followed by a 4.0 °C cooling into the present (Fig. 6e, Table 2). Both MBT/CBT records also have a 2 °C temperature oscillation between 30 and 22 ka.

The original East African MbrGDGTs calibration (Tierney et al., 2010) shows steady cooling of 0.9 °C from the LGM to the present (Fig. 7d, Table 2), while the global MbrGDGTs calibration (Pearson et al., 2011) reconstruction shows LGM and mid-Holocene temperatures differing by 3.1 °C, and LGM and present temperatures differing by 2.4 °C (Fig. 7e, Table 2). The global BSR (Pearson et al., 2011) calibration shows a steady cooling totaling 1.3 °C from the LGM to present (Fig. 8d, Table 2). Both the East African MbrGDGTs and the global BSR calibrations show an oscillation in temperature (2–3 °C) between 30 and 22 ka.

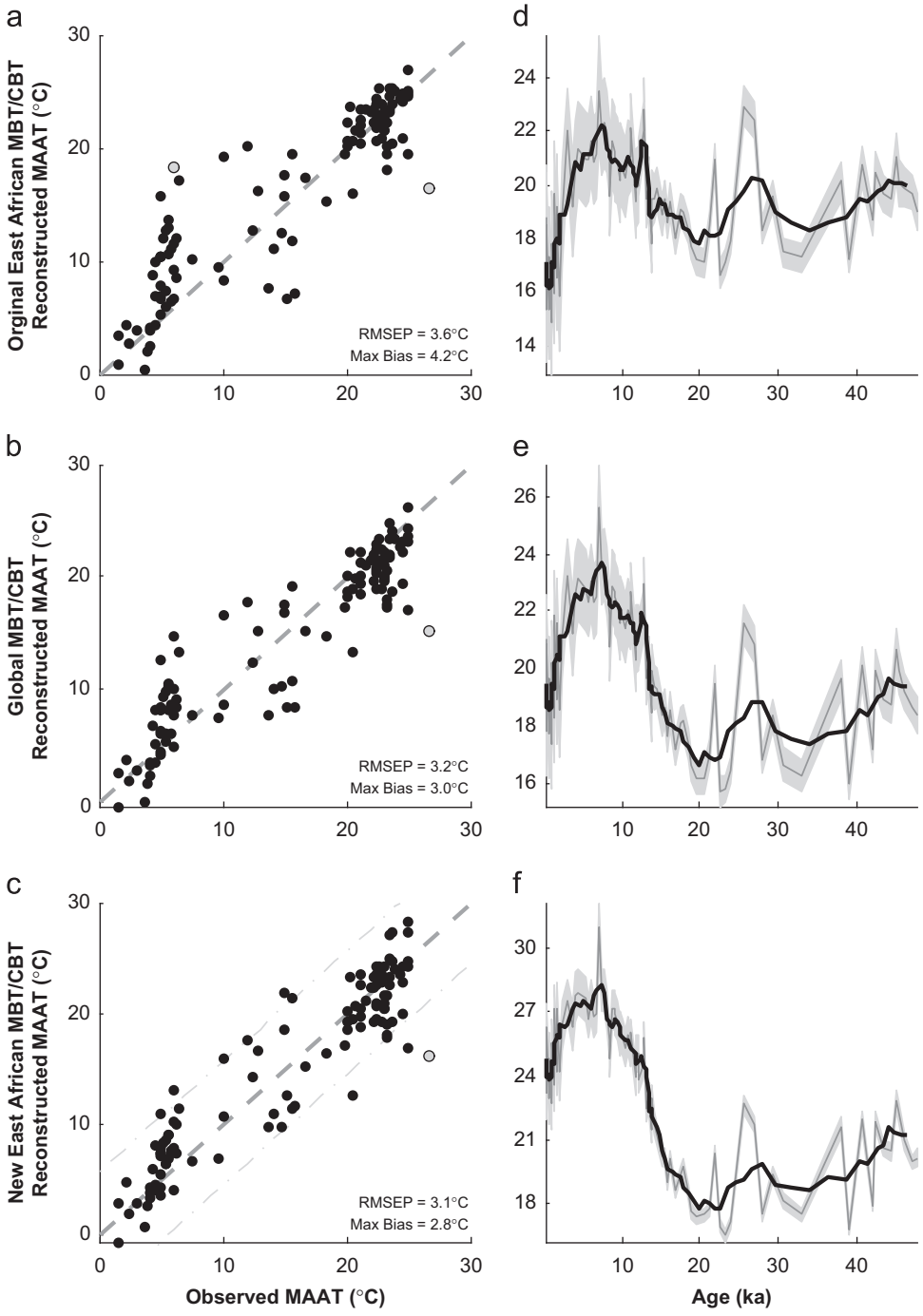

Fig. 6. Lacustrine MBT/CBT calibrations applied to our surface sediment dataset (left, (a)–(c)) and Sacred Lake (right, (d)–(f)). Surface sediment samples are plotted in black dots, with a 1:1 dashed gray line for reference. The dot-dashed line is the 95% confidence interval on the new East African calibration. Gray dots are outliers: Albert and Teleki for the original East African calibration and Lake Albert for both the global and new East African calibrations. For the Sacred Lake reconstructions, the thin gray line is the raw data, the thick black line is a 5-point running mean, and the light gray band is the 1σ error bootstrap error.

3.4. Development of new brGDGT calibrations

We have developed three new lacustrine brGDGT temperature calibrations from our expanded East African lakes dataset. To test the efficacy of existing calibration model types, we use previously published calibration methods (including the MBT/CBT and MbrGDGT methods), as well as another regression method that has not yet been applied to brGDGTs.

As expected, the new East African MBT/CBT calibration:

$$\mathrm{MAAT} = 2.54 + 45.28 \times \mathrm{MBT} - 5.02 \times \mathrm{CBT} \quad (10)$$

minimizes error when applied to the calibration dataset compared to the other lacustrine MBT/CBT calibrations ($r^2 = 0.87$, RMSE = 2.8 °C, RMSEP = 3.1 °C, max bias = 2.8 °C; Fig. 6c, Table 2), but we still see the greatest error in MAAT reconstruction in lakes $_{<16}$. The new East African MbrGDGT calibration:

$$\mathrm{MAAT} = 36.90 - 50.14 \times f(\mathbf{III}) - 35.52 \times f(\mathbf{II}) - 0.96 \times f(\mathbf{I}) \quad (11)$$

again, as expected, has lower error than the other MbrGDGT calibrations ($r^2 = 0.88$, RMSE = 2.7 °C, RMSEP = 3.1 °C, max bias = 3.2 °C; Fig. 7c, Table 2); however, this model, like the new MBT/CBT model, still has increased error at lake $_{<16}$ sites.

Table 2
Model statistics, including r^2, overall RMSE (°C), RMSE for lakes$_{<16}$ (°C), RMSE for lakes$_{>16}$ (°C), and RMSEP (°C), and ΔT (°C) from the LGM to mid-Holocene, mid-Holocene to present, and LGM to present for the five previously published and the four new East African lacustrine brGDGT temperature calibrations. r^2 and overall RMSE values for previously published calibrations are from the literature, while RMSE for lakes$_{<16}$, RMSE for lakes$_{>16}$, RMSEP, and max bias were calculated from the application of these calibrations to our surface sediment dataset. RMSEP of our new calibrations were calculated from the bootstrap error on the surface sediment dataset.

Calibration	r^2	RMSE	RMSE lakes$_{<16}$	RMSE lakes$_{>16}$	RMSEP	Max bias	ΔT: LGM to mid-Holocene	ΔT: Mid-Holocene to present	ΔT: LGM to present
Original East African MBT/CBT	0.89[a]	3.0[a]	4.7	2.0	3.6	4.2	3.8	−4.8	−1.1
Global MBT/CBT	0.62[b]	5.2[b]	3.6	2.8	3.2	3.0	6.6	−4.0	2.6
New East African MBT/CBT	0.87	2.8	3.2	2.8	3.1	2.8	10.4	−3.4	7.0
Original East African MbrGDGTs	0.94[a]	2.2[a]	3.8	2.2	3.0	3.7	−0.4	−0.5	−0.9
Global MbrGDGTs	0.84[c]	2.4[c]	5.9	2.3	4.4	6.8	3.1	−0.7	2.4
New East African MbrGDGTs	0.88	2.7	3.5	2.2	3.1	3.2	9.5	−0.8	8.6
Global BSR	0.88[c]	2.0[c]	6.1	3.8	5.1	6.6	0.5	−1.7	−1.3
East African SFS	0.94	1.9	1.9	2.0	2.1	1.0	6.3	−1.2	5.1

[a] From Tierney et al. (2010).
[b] From Sun et al. (2011).
[c] From Pearson et al. (2011).

Our final new calibration was developed using stepwise forward selection (SFS). We started with f(**III**), as it has the highest correlation with MAAT, and added one brGDGT at a time, utilizing the one that improved the regression the most. Between each step, we performed an F-test on the significance of adding each variable, stopping when the addition no longer produced a significant decrease in error (Hocking, 1976). Since SFS makes the sometimes incorrect assumption that variables picked initially are part of the optimal regression, we regressed every possible subset of brGDGTs against MAAT, selecting the optimal regression for each number of variables. Results for SFS and all possible regressions were the same when utilizing three or more brGDGTs. SFS, verified by all possible regressions, determined that the optimal regression contained four brGDGTs, resulting in the following calibration:

$$\mathrm{MAAT} = 22.77 - 33.58 \times f(\mathbf{III}) - 12.88 \times f(\mathbf{II}) - 418.53 \times f(\mathbf{IIc}) + 86.43 \times f(\mathbf{Ib}) \quad (12)$$

The SFS calibration improves both the accuracy and error of prediction over the MBT/CBT and MbrGDGT calibrations (r^2=0.94, RMSE=1.9 °C, RMSEP=2.1 °C, max bias=1.0 °C; Fig. 8c, Table 2). Moreover, this is the only calibration that has uniform error across the dataset, including lakes$_{<16}$.

3.5. Application of the new brGDGT calibrations to Sacred Lake

All of our new East African brGDGT calibrations reconstruct similar patterns of temperature change in the Sacred Lake core, but the amplitude varies between the LGM and present and the mid-Holocene and present. Our new East African MBT/CBT reconstruction shows large warming from the LGM to the mid-Holocene (ΔT=10.4 °C), and cooling of 3.4 °C from the mid-Holocene to the present, resulting in 7.0 °C warming from LGM to present (Fig. 6f, Table 2). The new East African MbrGDGT reconstruction shows a similar magnitude of warming (9.5 °C) from the LGM to the mid-Holocene, a slight cooling of 0.8 °C into the present, with an overall warming of 8.6 °C from the LGM to present (Fig. 7f, Table 2). Application of the SFS calibration to the Sacred Lake data shows a warming of 6.3 °C from the LGM to the mid-Holocene, followed by a cooling of 1.2 °C, resulting in a 5.1 °C warming between the LGM and present (Fig. 8d, Table 2). The SFS calibration is the only calibration, new or previously published, that does not demonstrate a 2–3 °C warm pulse between 30 and 22 ka.

4. Interpretive context

Paleotemperature proxies must have low error statistics and produce accurate temperatures downcore before they can be considered reliable. Accuracy is relatively easy to assess in surface sediments, but to evaluate a calibration's accuracy in a paleoclimate context, we need other paleotemperature reconstructions for comparison. While there are relatively few paleotemperature records from tropical Africa, existing datasets do share common features, such as warming from the LGM to present, that allow us to develop a target of expected temperature changes in our Sacred Lake core. Here we outline two main features in previously published paleotemperature records: the overall amplitude of warming between the LGM and present and the magnitude of cooling between the mid-Holocene and present.

Temperature reconstructions from low elevations ($<$1000 m asl) in tropical Africa are primarily derived from GDGTs. The TEX_{86} proxy (Schouten et al., 2002) was used to reconstruct lake surface temperatures (LSTs) from Lakes Malawi (Powers et al., 2005) and Tanganyika (Tierney et al., 2008), and documented LGM-present warming of 3.4 and 2.9 °C, respectively. Similarly, reconstructed temperatures from soil-derived brGDGTs in a sediment core in the Congo River delta showed warming of 3.7 °C from the LGM to present (Weijers et al., 2007a).

These data suggest LGM-present warming of 3–4 °C, consistent with recent global syntheses of tropical temperature history (Shakun and Carlson, 2010). However, paleotemperature reconstructions from higher elevations in tropical Africa tend to show higher amplitude LGM-present warming than in the lower elevation sites (Farrera et al., 1999). Pollen based estimates show that LGM temperatures were approximately 5.1 °C cooler at Sacred Lake (van Zinderen Bakker and Coetzee, 1972) and 4 ± 2 °C cooler at similar elevations (2240 m asl) in Burundi (Bonnefille et al., 1990). Several other pollen records document montane taxa 1000–1500 m below their present minimum altitudes (Coetzee, 1967), suggesting temperatures 6–9 °C cooler based upon modern temperature lapse rates. Glacial moraines also suggest significantly cooler temperatures at the LGM, with ELAs depressed by 620 to 1020 m across East Africa. The largest depression occurs on the eastern flank of Mt. Kenya (Porter, 2001), the location of Sacred Lake, which would have been 4–8 °C cooler than present day (Mark et al., 2005). These estimates do assume that lapse rates and other environmental parameters that affect vegetation

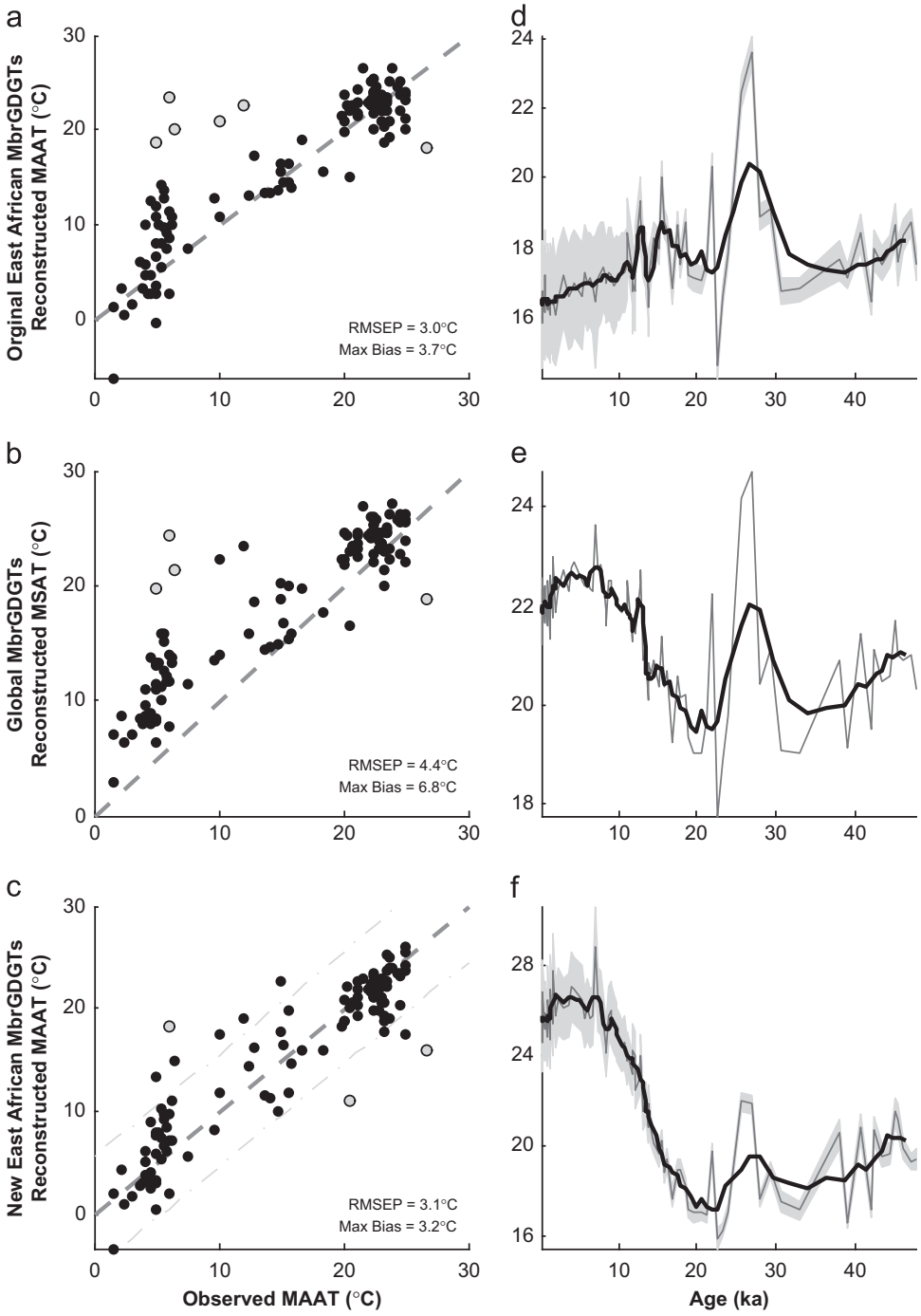

Fig. 7. MbrGDGTs calibrations applied to our surface sediment dataset (left, (a)–(c)) and Sacred Lake (right, (d)–(f)). Surface sediment samples are plotted in black dots, with a 1:1 dashed gray line for reference. The dot-dashed line is the 95% confidence interval on the new East African calibration. Gray dots are outliers: Ellis, Albert, Rutundu, Hohnell, Nanyuki, and Teleki for the original East African calibration; Albert, Hohnell, Nanyuki, and Teleki for the global calibration; Mahuhura, Albert, and Teleki for the new East African calibration. For the Sacred Lake reconstructions, the thin gray line is the raw data, the thick black line is a 5-point running mean, and the light gray band is the 1σ error bootstrap error.

and glacier mass balance, including precipitation, cloudiness, albedo, CO_2, and humidity, remained constant through time.

Existing reconstructions also suggest changes in temperature between the mid-Holocene and present in many East African records. TEX_{86} reconstructions from Lakes Tanganyika (Tierney et al., 2008) and Malawi (Powers et al., 2005) document cooling from ~5000 yr BP to the present, with amplitudes ranging from 1 to 2 °C. Both Coetzee (1967) and Livingstone (1967) note the presence of a climatic optimum in pollen reconstructions from Mt. Kenya (including Sacred Lake) and the Rwenzori Mountains, although they do not give quantitative estimates of temperature change.

While these data do exhibit considerable variation, there are common patterns that we use to qualitatively investigate the performance of brGDGT calibrations. Low elevation, LGM-present temperature reconstructions of ~3–4 °C, combined with high elevation reconstructions of up to 8 °C suggest that Sacred Lake should have experienced temperature changes between these two end members given its mid altitude (2350 m asl) position. We expect that Sacred Lake would show a temperature decrease

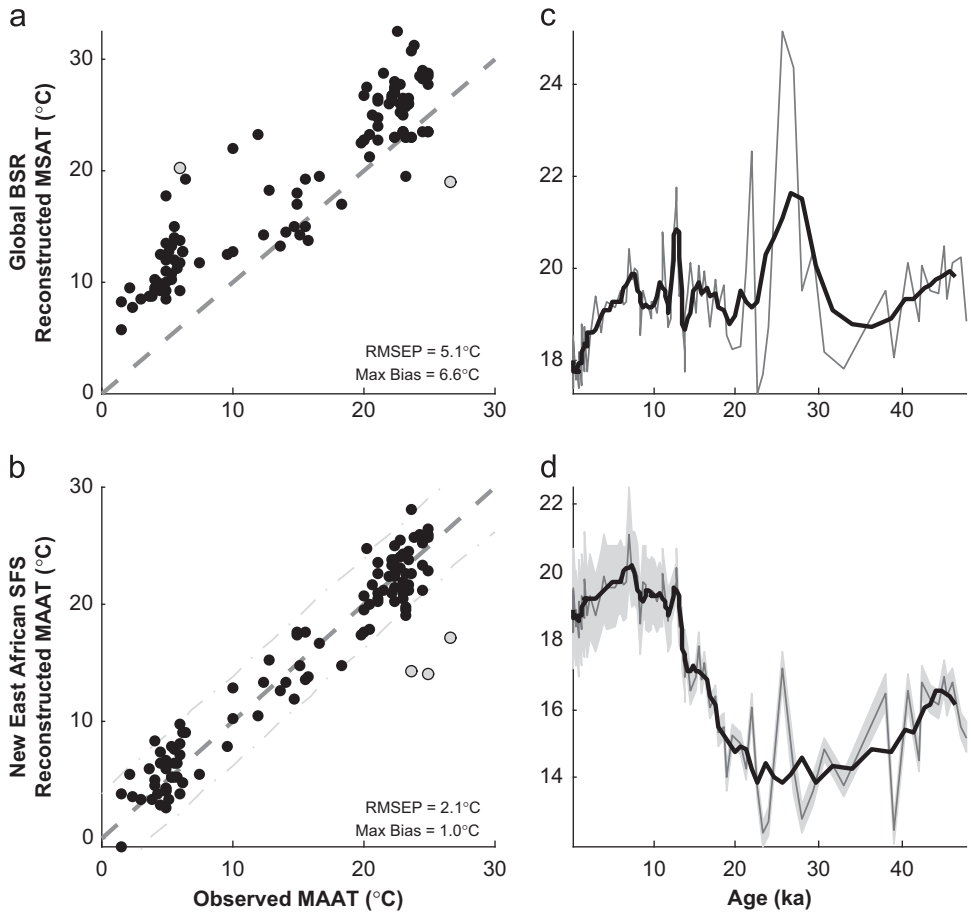

Fig. 8. Subsets regression calibrations applied to our surface sediment dataset (left, (a)–(b)) and Sacred Lake (right, (c)–(d)). Surface sediment samples are plotted in black dots, with a 1:1 dashed gray line for reference. The dot-dashed line is the 95% confidence interval on the new East African calibration. Gray dots are outliers: Albert and Teleki for BSR; Edward, Nyungu, Tanganyika, and Albert for SFS. For the Sacred Lake reconstructions, the thin gray line is the raw data, the thick black line is a 5-point running mean, and the light gray band is the 1σ error bootstrap error.

between 0 and 2 °C between the mid-Holocene and present, within the range of previous reconstructions, and we expect the present to be warmer than the LGM. Below, we examine the ability of the different reconstructions to generate these patterns.

5. Discussion

We apply both previously published (Pearson et al., 2011; Sun et al., 2011; Tierney et al., 2010) and new temperature calibrations based upon lacustrine brGDGT distributions reported by Tierney et al. (2010; 41 lakes) and our new dataset (70 lakes; Tables A1 and A3) and core samples from Sacred Lake. Together, these allow us to evaluate the performance of published calibrations in response to temperature gradients in both space (through our new calibration set) and time (in our sediment core).

All brGDGT calibrations capture the general patterns of warm vs. cold lakes in our surface sediment dataset. However, there are large differences in their accuracy, precision, and bias in the performance of the models at low temperatures. Most calibrations produce qualitatively similar patterns of temperature changes when applied to our core from Sacred Lake, but the amplitudes vary considerably, and a few reconstructions even show decreasing temperatures between the LGM and present.

We recognize that application of these models to a single lake core does not conclusively validate nor invalidate the different brGDGT calibrations; however, the performance of different calibration types (MBT/CBT, MbrGDGTs, etc.) on both our surface sediment dataset and the Sacred Lake core lends insight into the response of brGDGTs to environmental gradients as well as the optimal methods for temperature calibration.

5.1. MBT/CBT calibrations

The global soils MBT/CBT calibration has a cold bias in reconstructed MAAT, as was found in previous studies of lacustrine brGDGTs (Pearson et al., 2011; Sun et al., 2011; Tierney et al., 2010; Tierney and Russell, 2009), but the previously published lacustrine MBT/CBT calibrations reconstruct modern MAAT more accurately than other types of previously published lacustrine calibrations, as indicated by relatively low RMSEP and low systematic bias when applied to our surface sediment dataset. However, the MBT/CBT calibrations, including our new East African MBT/CBT calibration, have large errors in colder lakes, where pH variability is highest. Furthermore, all MBT/CBT calibrations fail to reconstruct reasonable temperature change when applied to the Sacred Lake core samples (Fig. 6d–f). Previously published East African paleotemperature reconstructions and global syntheses indicate that temperatures have increased from the LGM to present. Application of the original East African MBT/CBT calibration (Tierney et al., 2010) to our Sacred Lake core suggests LGM to present cooling. Application of the global lakes MBT/CBT calibration (Sun et al., 2011) estimates LGM-present warming to be 2.6 °C, but also has a 4 °C cooling from the mid-Holocene to the present, much larger than previous estimates (e.g., Tierney et al., 2008; Weijers et al., 2007a).

The new East African MBT/CBT calibration reconstructs deglacial warming >10 °C, much higher than all previous African estimates and comparable to temperature changes estimated for Greenland (Shakun and Carlson, 2010).

The varying amplitudes of temperature change in these reconstructions are dictated by the relative importance of MBT and CBT in each of the equations. The high relative importance of CBT to MBT in the original East African lakes MBT/CBT calibration (Tierney et al., 2010) results in a very strong cooling from the mid-Holocene to present, as CBT values continue to increase while MBT values remain fairly constant. Conversely, the low relative importance of CBT to MBT in the new East African lakes calibration results in less cooling from the mid-Holocene to present. Even with a relatively large (111-sample) and well-constrained calibration dataset, free from the effects of seasonality of temperature, we have difficulty parameterizing the MBT/CBT equations. This is likely due to the fact that CBT only utilizes brGDGTs **I**, **Ib**, **II**, and **IIb**, neglecting the group **III** brGDGTs and brGDGTs with two cyclopentyl rings, which we find to be significant for parameterizing temperature in our SFS calibration.

5.2. MbrGDGTs calibrations

Previously published MbrGDGT calibrations have high RMSEP values when applied to our surface sediment dataset, particularly at lake$_{<16}$ sites. Misfit is even higher than it was for the MBT/CBT calibrations, with a systematic bias towards overestimated temperatures in the colder lakes. Unlike MBT/CBT, however, the MbrGDGT calibrations differ both qualitatively and quantitatively in their reconstruction of East African temperature. The original East African MbrGDGT reconstruction shows steady cooling from the LGM into the present (Fig. 7d, Table 2), inconsistent with all existing temperature records from Africa. The new East African MbrGDGT calibration reconstructs temperature changes of 8.6 °C (Fig. 7f, Table 2), substantially higher than most estimates of LGM to present warming from the tropics (Shakun and Carlson, 2010). The global MbrGDGT calibration reconstructs a more modest 2.4 °C warming between the LGM and present at Sacred Lake. While we would expect a higher amplitude of warming at the elevation of Sacred Lake, this reconstruction is within the reasonable limits of LGM to present temperature change compared to previously published records. However, we caution its use on cores from East Africa, as it tends to overestimate MAAT in surface sediments found in lakes$_{<16}$ (see Section 5.3 for further discussion).

The MbrGDGT method is based upon the assumption that the degree of branching is more strongly related to temperature than is the degree of cyclization. Our data support this finding; however, our data also suggest that an accurate brGDGT temperature calibration must involve both acyclic and cyclic brGDGTs in order to accurately reconstruct temperature. Weijers et al. (2007b) postulated that the degree of cyclization of brGDGTs results from microbial regulation of proton gradients across the cell membrane, and the degree of methylation is controlled by both the MAAT and pH of the environment. If we accept that variability in cyclization is indeed caused by changes in pH, a pH-driven increase in cyclization would also cause a change in the fluidity of the membrane. However, differences in MAAT at a given pH could result in sub-optimal permeability with abundances of cyclopentyl moieties that were set solely by pH. This fluidity is then optimized by changes in methylation. Thus, it is a combination of both cyclization and methylation of brGDGTs that determine the optimal fluidity of the membrane at different temperatures. This is why MBT and CBT were used in the original soils calibration (Weijers et al., 2007b). In essence, we suggest that the lack of cyclized compounds in the MbrGDGT calibrations limits their applicability, as they are unable to capture the optimal membrane fluidity for a given temperature, which is achieved through a combination of (pH-induced) cyclopentane rings and methyl branches. This is likely the reason for the inaccurate reconstruction of paleotemperature in Sacred Lake, as both diatom (Street-Perrott et al., 1997) and brGDGT evidence show a gradual change from alkaline to more acidic lacustrine conditions from the LGM to present.

5.3. Subsets regression calibrations

The global BSR calibration does not accurately estimate temperatures in either our surface sediment dataset or Sacred Lake. This calibration shows substantial bias at cold sites in our surface sediment dataset, and estimates net cooling from the LGM to present in Sacred Lake. The large RMSEP and max bias in our surface sediment dataset results from both a large variance in the reconstructed MAAT data at all temperatures and a systematic positive offset of reconstructed MAAT in colder lakes. Pearson et al. (2011) calibrated their BSR dataset to MSAT rather than MAAT. Calibration to MSAT assumes that the microbes producing brGDGTs are most active during the period of peak photosynthetic activity in summer. The seasonality of brGDGT producers in lakes is poorly constrained; however, brGDGTs in soils have been shown to record MAAT with little seasonal bias (Weijers et al., 2011, 2007b). Isotopic (Weijers et al., 2010), environmental (Weijers et al., 2006), and culture data (Sinninghe Damsté et al., 2011) suggest that brGDGTs are likely derived from heterotrophic, and potentially facultative anaerobic, members of the Acidobacteria, and therefore could live during all seasons. Assuming that the bacteria producing brGDGTs are active year-round, we argue that calibration of brGDGTs to summer temperature in temperate-zone to high-latitude lakes in the Pearson et al. (2011) dataset will likely result in overestimation of temperature in our cold lakes, which are largely high-elevation, polymictic lakes with little to no thermal seasonality. Our limited understanding of the impacts of seasonality on brGDGT calibrations highlights the need for sediment trap studies to investigate the seasonality of production of brGDGTs in the lacustrine environment.

We investigated many different calibrations using subsets of the nine brGDGTs calibrated to MAAT, including linear and non-linear regressions of various subsets of the data and paleoecological transfer function approaches (Birks, 1998 and references therein), but none of these non-linear methods performed as well as the SFS calibration, which best captures the variance in our surface sediment dataset and provides a credible temperature history when applied to Sacred Lake, with LGM to present warming of 5.1 °C (Fig. 6e and f, Table 2). This warming slightly exceeds estimated temperature changes observed at low elevations in the East African tropics but is the same as pollen-based reconstructions from Sacred Lake and is close to the temperatures estimated from ELAs on Mt. Kenya and, therefore, seems most realistic. The RMSEP of the SFS calibration is lower than any of the other calibrations and does not have increased misfit at lake$_{<16}$ sites, which we believe comes from its ability to deconvolve temperature and pH effects in the dataset.

The SFS calibration relies upon four brGDGTs, including **IIc**, which is often found in relatively low abundance (Table A3), making it more difficult to quantify accurately. However, if we were to exclude **IIc** from our calibration, the RMSE of the SFS calibration rises from 1.9 to 3.1 °C, with increased misfit in lakes$_{<16}$. Furthermore, **IIc** shows up in our regression when using only three variables in the calibration, making it more important to our calibration than **II**, which is introduced only when using four variables. This would imply that **IIc** is very important in deconvolving the effects of pH, or another

environmental variable, from temperature in our calibration. Tierney et al. (2010) postulated that depth may be a primary control on the abundance of **IIc**. We find, however, that **IIc** is not significantly correlated to depth in our lakes$_{<16}$ dataset but does show a significant correlation with pH (Table 1). While all three mono-cyclic brGDGTs do have a higher correlation with pH, it is possible that this variability is accounted for by the inclusion of **Ib**, and **IIc** is further adjusting for pH, or some yet unexplored environmental variable.

5.4. Applicability of the SFS calibration outside of East Africa

We demonstrate that the SFS calibration most accurately reconstructs modern and past MAAT in East Africa, but its applicability outside the region remains unknown. Based upon the misfit of the BSR calibrations, which were calibrated to MSAT (Pearson et al., 2011), when applied to our dataset, we surmise that the seasonality of temperature and perhaps lake mixing regime could play a critical role in determining the applicability of our calibration outside of the tropics. While this is not a problem in East Africa due to the lack of thermal seasonality, seasonality does have the potential to cause inaccurate MAAT reconstructions in temperate and arctic regions if brGDGTs are produced during a particular season. The global BSR calibration has a large offset at low MAAT when applied to our East African surface sediment dataset, and negligible offset at warmer MAAT (Fig. 8b). This low temperature offset is consistent with the offset of MSAT vs. MAAT in high vs. low latitude environments, as higher latitudes tend to have a lower MAAT combined with a larger difference between MAAT and MSAT. Thus, the brGDGTs produced at higher elevations in East Africa likely have similar distributions to those at higher latitude in the global BSR surface sediment data, where MAAT is comparable but MSAT is not. If these two environments do indeed produce similar brGDGT distributions, the SFS calibration should accurately reconstruct MAAT at higher latitude locations outside of East Africa. Application to both other tropical and extra-tropical locations is needed to test if the SFS calibration is regional or can be applied globally to accurately reconstruct MAAT in surface and core sediments.

5.5. Implications of the Sacred Lake reconstruction

Our new SFS calibration and previous pollen estimates show an identical 5.1 °C LGM to present warming at Sacred Lake, Mt. Kenya. Moreover, our continuous brGDGT derived temperature record has many similarities to existing TEX_{86} temperature reconstructions from Lakes Malawi and Tanganyika, East Africa (Powers et al., 2005; Tierney et al., 2008) including a cool LGM, deglacial warming beginning ~20 ka, abrupt warming ca. 12.5 ka, and a mid-Holocene thermal maximum. We infer a slightly higher LGM to present warming than in the Congo Basin (Weijers et al., 2007a) and Lakes Malawi and Tanganyika, which could reflect the amplification of deglacial warming at higher altitude (Bradley et al., 2006).

The majority of deglacial warming occurs between 18 and 11 ka, and roughly follows a pattern set by radiative forcing from greenhouse gases. However, both early deglacial warming at ~20 ka and the mid-Holocene thermal maximum occur during local minima in greenhouse gas radiative forcing, requiring other processes to transmit heat into the tropical African atmosphere. We speculate that early warming in tropical Africa represents a remote response to changes in northern hemisphere glaciers, perhaps related to planetary albedo. Given the dramatic changes in African hydrology during the mid-Holocene, this warming likely reflects coupled reorganizations of surface temperatures, precipitation, and cloud cover.

Notably, our new temperature record from Sacred Lake bears little resemblance to records of clastic sediment inputs to Sacred Lake (Olago et al., 2001). Increased clastic fluxes would presumably indicate soil-derived inputs, including soil derived brGDGTs. This dissimilarity suggests that soil-derived brGDGTs have little impact on temperature reconstructions, at least in Sacred Lake. Rather, the coherent temperature variability in this dataset, including abrupt changes, strongly suggests that brGDGTs record changes in air and lake water temperatures. This finding bodes well for future application of brGDGTs to temperature reconstructions using lacustrine sediments.

6. Conclusions

We show that the relative distributions of brGDGTs in tropical lakes indeed have a strong correlation with MAAT, and we demonstrate, for the first time, that they can be applied to reconstruct a credible temperature history from a small tropical lake. Our inter-calibration comparison highlights difficulties in separating the influence of temperature from other environmental controls, notably pH, and suggests that the most accurate and precise reconstructions will likely derive from calibrations based upon a subset of brGDGTs strongly controlled by temperature combined with a subset mainly controlled by other environmental variables that can deconvolve the influence of other environmental controls on brGDGT distributions.

We find that regional calibrations of brGDGTs perform better than global brGDGT calibrations when reconstructing temperatures on both surface sediments and the Sacred Lake core, suggesting that lakes may require regional calibration. In light of the warm bias that results from application of calibrations that use summer temperature as a calibration target in north temperate lakes, we speculate that the regional response of brGDGTs could be related to latitudinal variations in lake mixing and associated changes in the seasonality of brGDGT production. If so, this could also explain prior results that showed that regional calibrations can improve brGDGT calibrations in tropical soil setting (Sinninghe Damsté et al., 2008).

Acknowledgements

This work was conducted with funds from ACS-PRF grant 49235-DNI2. The research leading to these results has received funding from the European Research Council under the European Union's Seventh Framework Programme (FP7/2007-2013)/ERC grant agreement no. [226600]. We thank Rafael Tarozo (Brown), Jort Ossebaar (NIOZ), and Ellen Hopmans (NIOZ) for assistance in the laboratory. We would also like to thank Joe Werne and Steve Juggins for comments that helped to improve this manuscript.

Appendix A. Supporting information

Supplementary data associated with this article can be found in the online version at http://dx.doi.org/10.1016/j.epsl.2012.09.031.

References

Berke, M.A., Johnson, T.C., Werne, J.P., Schouten, S., Sinninghe-Damsté, J.S., 2012. A mid-Holocene thermal maximum at the end of the African Humid Period. Earth Planet. Sci. Lett. 351–352, 95–104.

Birks, H.J.B., 1998. Numerical tools in paleolimnology—Progress, potentialities, and problems. J. Paleolimnol. 20, 307–332.

Blaga, C.I., Reichart, G.J., Schouten, S., Lotter, A.F., Werne, J.P., Kosten, S., Mazzeo, N., Lacerot, G., Sinninghe Damsté, J.S., 2010. Branched glycerol dialkyl glycerol tetraethers in lake sediments: can they be used as temperature and pH proxies? Org. Geochem. 41, 1225–1234.

Bonnefille, R., Roeland, J.C., Guiot, J., 1990. Temperature and rainfall estimates for the past 40,000 years in equatorial Africa. Nature 346, 347–349.

Bradley, R.S., Vuille, M., Diaz, H.F., Vergara, W., 2006. Threats to water supplies in the tropical Andes. Science 312, 1755–1756.
Coetzee, J.A., 1967. Pollen analytical studies in East and southern Africa. Palaeoecol. Africa 3, 1–146.
Efron, B., 1979. Bootstrap methods: another look at the Jackknife. Ann. Stat. 7, 1–26.
Eggermont, H., Heiri, O., Russell, J., Vuille, M., Audenaert, L., Verschuren, D., 2010. Paleotemperature reconstruction in tropical Africa using fossil Chironomidae (Insecta: Diptera). J. Paleolimnol. 43, 413–435.
Farrera, I., Harrison, S.P., Prentice, I.C., Ramstein, G., Guiot, J., Bartlein, P.J., Bonnefille, R., Bush, M., Cramer, W., von Grafenstein, U., Holmgren, K., Hooghiemstra, H., Hope, G., Jolly, D., Lauritzen, S.E., Ono, Y., Pinot, S., Stute, M., Yu, G., 1999. Tropical climates at the Last Glacial Maximum: a new synthesis of terrestrial palaeoclimate data. I. Vegetation, lake levels and geochemistry. Clim. Dyn. 15, 823–856.
Fawcett, P.J., Werne, J.P., Anderson, R.S., Heikoop, J.M., Brown, E.T., Berke, M.A., Smith, S.J., Goff, F., Donohoo-Hurley, L., Cisneros-Dozal, L.M., Schouten, S., Sinninghe Damsté, J.S., Huang, Y.S., Toney, J., Fessenden, J., WoldeGabriel, G., Atudorei, V., Geissman, J.W., Allen, C.D., 2011. Extended megadroughts in the southwestern United States during Pleistocene interglacials. Nature 470, 518–521.
Gasse, F., Chalie, F., Vincens, A., Williams, M.A.J., Williamson, D., 2008. Climatic patterns in equatorial and southern Africa from 30,000 to 10,000 years ago reconstructed from terrestrial and near-shore proxy data. Quat. Sci. Rev. 27, 2316–2340.
Heegaard, E., Birks, H.J.B., Telford, R.J., 2005. Relationships between calibrated ages and depth in stratigraphical sequences: an estimation procedure by mixed-effect regression. Holocene 15, 612–618.
Hocking, R.R., 1976. The analysis and selection of variables in linear-regression. Biometrics 32, 1–49.
Huguet, C., Hopmans, E.C., Febo-Ayala, W., Thompson, D.H., Sinninghe Damsté, J.S., Schouten, S., 2006. An improved method to determine the absolute abundance of glycerol dibiphytanyl glycerol tetraether lipids. Org. Geochem. 37, 1036–1041.
Kulongoski, J.T., Hilton, D.R., Selaolo, E.T., 2004. Climate variability in the Botswana Kalahari from the late Pleistocene to the present day. Geophys. Res. Lett., 31.
Livingstone, D.A., 1967. Postglacial vegetation of the Ruwenzori Mountains in equatorial Africa. Ecol. Monogr. 37, 25–52.
Loomis, S.E., Russell, J.M., Sinninghe Damsté, J.S., 2011. Distributions of branched GDGTs in soils and lake sediments from western Uganda: implications for a lacustrine paleothermometer. Org. Geochem. 42, 739–751.
Mark, B.G., Harrison, S.P., Spessa, A., New, M., Evans, D.J.A., Helmens, K.F., 2005. Tropical snowline changes at the last glacial maximum: a global assessment. Quat. Int. 138, 168–201.
McGregor, G.R., Nieuwolt, S., 1998. Tropical Climatology, second ed. John Wiley & Sons, Chichester.
Olago, D.O., Street-Perrott, F.A., Ivanovich, M., Harkness, D.D., 2001. U/Th and ^{14}C isotope dating of lake sediments from Sacred Lake and Lake Nkunga, Kenya. Afr. J. Sci. Technol. 2, 36–46.
Pearson, E.J., Juggins, S., Talbot, H.M., Weckstrom, J., Rosen, P., Ryves, D.B., Roberts, S.J., Schmidt, R., 2011. A lacustrine GDGT-temperature calibration from the Scandinavian Arctic to Antarctic: renewed potential for the application of GDGT-paleothermometry in lakes. Geochim. Cosmochim. Acta 75, 6225–6238.
Peterse, F., Prins, M.A., Beets, C.J., Troelstra, S.R., Zheng, H., Gu, Z., Schouten, S., Sinninghe Damsté, J.S., 2011. Decoupled warming and monsoon precipitation in East Asia over the last deglaciation. Earth Planet. Sci. Lett. 301, 256–264.
Porter, S.C., 2001. Snowline depression in the tropics during the Last Glaciation. Quat. Sci. Rev. 20, 1067–1091.
Powers, L., Werne, J.P., Vanderwoude, A.J., Sinninghe Damsté, J.S., Hopmans, E.C., Schouten, S., 2010. Applicability and calibration of the TEX_{86} paleothermometer in lakes. Org. Geochem. 41, 404–413.
Powers, L.A., Johnson, T.C., Werne, J.P., Castanada, I.S., Hopmans, E.C., Sinninghe Damsté, J.S., Schouten, S., 2005. Large temperature variability in the southern African tropics since the Last Glacial Maximum. Geophys. Res. Lett. 32, L08706.
Schouten, S., Hopmans, E.C., Schefuss, E., Sinninghe Damsté, J.S., 2002. Distributional variations in marine crenarchaeotal membrane lipids: a new tool for reconstructing ancient sea water temperatures? Earth Planet. Sci. Lett. 204, 265–274.
Shakun, J.D., Carlson, A.E., 2010. A global perspective on Last Glacial Maximum to Holocene climate change. Quat. Sci. Rev. 29, 1801–1816.
Sinninghe Damsté, J.S., Ossebaar, J., Abbas, B., Schouten, S., Verschuren, D., 2009. Fluxes and distribution of tetraether lipids in an equatorial African lake: constraints on the application of the TEX_{86} palaeothermometer and BIT index in lacustrine settings. Geochim. Cosmochim. Acta 73, 4232–4249.
Sinninghe Damsté, J.S., Ossebaar, J., Schouten, S., Verschuren, D., 2008. Altitudinal shifts in the branched tetraether lipid distribution in soil from Mt. Kilimanjaro (Tanzania): implications for the MBT/CBT continental palaeothermometer. Org. Geochem. 39, 1072–1076.
Sinninghe Damsté, J.S., Ossebaar, J., Schouten, S., Verschuren, D., 2012. Distribution of tetraether lipids in the 25-ka sedimentary record of Lake Challa: extracting reliable TEX_{86} and MBT/CBT palaeotemperatures from an equatorial African lake. Quat. Sci. Rev. 50, 43–54.
Sinninghe Damsté, J.S., Rijpstra, W.I.C., Hopmans, E.C., Weijers, J.W.H., Foesel, B.U., Overman, J., Dedysh, S.N., 2011. 13,16-Dimethyl octacosanedionic acid (*iso*-diabolic acid): a common membrane-spanning lipid of *Acidobacteria* subdivisions 1 and 3. Appl. Environ. Microbiol. 77, 4147–4154.
Street-Perrott, F.A., Huang, Y.S., Perrott, R.A., Eglinton, G., Barker, P., BenKhelifa, L., Harkness, D.D., Olago, D.O., 1997. Impact of lower atmospheric carbon dioxide on tropical mountain ecosystems. Science 278, 1422–1426.
Stuiver, M., Reimer, P.J., 2010. CALIB 6.0.
Stute, M., Talma, A.S., 1998. Glacial temperatures and moisture transport regimes reconstructed from noble gases and $\delta^{18}O$, Stampriet aquifer, Namibia, Isotope Techniques in the Study of Environmental Change: Proceedings of a Symposium in Vienna. IAEA, Vienna, pp. 307–318.
Sun, Q., Chu, G., Liu, M., Xie, M., Li, S., Ling, Y., Wang, X., Shi, L., Jia, G., Lü, H., 2011. Distributions and temperature dependence of branced glycerol dialkyl glycerol tetraethers in recent lacustrine sediments from China and Nepal. J. Geophys. Res. 116, G01008.
ter Braak, C.J.F., Juggins, S., 1993. Weighted averaging partial least-squares regression (WA-PLS): an improved method for reconstructing environmental variables from species assemblages. Hydrobiologia 269, 485–502.
Tierney, J.E., Russell, J.M., 2009. Distributions of branched GDGTs in a tropical lake system: implications for lacustrine application of the MBT/CBT paleoproxy. Org. Geochem. 40, 1032–1036.
Tierney, J.E., Russell, J.M., Eggermont, H., Hopmans, E.C., Verschuren, D., Sinninghe Damsté, J.S., 2010. Environmental controls on branched tetraether lipid distributions in tropical East African lake sediments. Geochim. Cosmochim. Acta 74, 4902–4918.
Tierney, J.E., Russell, J.M., Huang, Y.S., Sinninghe Damsté, J.S., Hopmans, E.C., Cohen, A.S., 2008. Northern hemisphere controls on tropical southeast African climate during the past 60,000 years. Science 322, 252–255.
van Zinderen Bakker, E.M., Coetzee, J.A., 1972. A re-appraisal of late-Quaternary climatic evidence from tropical Africa. Palaeoecol. Africa 7, 151–181.
Weijers, J.W.H., Bernhardt, B., Peterse, F., Werne, J.P., Dungait, J.A.J., Schouten, S., Sinninghe Damsté, J.S., 2011. Absence of seasonal patterns in MBT–CBT indices in mid-latitude soils. Geochim. Cosmochim. Acta 75, 3179–3190.
Weijers, J.W.H., Schefuss, E., Schouten, S., Sinninghe Damsté, J.S., 2007a. Coupled thermal and hydrological evolution of tropical Africa over the last deglaciation. Science 315, 1701–1704.
Weijers, J.W.H., Schouten, S., Hopmans, E.C., Geenevasen, J.A.J., David, O.R.P., Coleman, J.M., Pancost, R.D., Sinninghe Damsté, J.S., 2006. Membrane lipids of mesophilic anaerobic bacteria thriving in peats have typical archaeal traits. Environ. Microbiol. 8, 648–657.
Weijers, J.W.H., Schouten, S., van den Donker, J.C., Hopmans, E.C., Sinninghe Damsté, J.S., 2007b. Environmental controls on bacterial tetraether membrane lipid distribution in soils. Geochim. Cosmochim. Acta 71, 703–713.
Weijers, J.W.H., Wiesenberg, G.L.B., Bol, R., Hopmans, E.C., Pancost, R.D., 2010. Carbon isotopic composition of branched tetraether membrane lipids in soils suggest a rapid turnover and a heterotropic life style of their source organism(s). Biogeosci. Discuss. 7, 3691–3734.